

# Cost-Efficient Medium Frequency Propagation Research with Software Defined Radio

Casey M. Hess<sup>1\*</sup>, Sohail Anwar<sup>2</sup>

<sup>1</sup>Division of Business, Engineering, and Information Sciences and Technology, Department of Electromechanical Engineering Technology, Pennsylvania State University, Altoona Campus, Altoona, Pennsylvania, USA

<sup>2</sup>Division of Business, Engineering, and Information Sciences and Technology, Department of Engineering, Pennsylvania State University, Altoona Campus, Altoona, Pennsylvania, USA

Email: \*czh5808@psu.edu

**How to cite this paper:** Hess, C.M. and Anwar, S. (2024) Cost-Efficient Medium Frequency Propagation Research with Software Defined Radio. *World Journal of Engineering and Technology*, 12, 158-169.  
<https://doi.org/10.4236/wjet.2024.121010>

**Received:** December 21, 2023

**Accepted:** February 17, 2024

**Published:** February 20, 2024

Copyright © 2024 by author(s) and Scientific Research Publishing Inc.  
This work is licensed under the Creative Commons Attribution International License (CC BY 4.0).  
<http://creativecommons.org/licenses/by/4.0/>



Open Access

## Abstract

Medium Frequency radio holds significance in modern society as it supports broadcasting and individual communications in the public, government, and military sectors. Enhancing the availability and quality of these communications is only possible by enhancing the understanding of medium frequency propagation. While traditional methods of radio wave propagation research can have a high material demand and cost, software defined radio presents itself as a versatile and low-cost platform for medium frequency signal reception and data acquisition. This paper details a research effort that utilizes software defined radio to help characterize medium frequency signal strength in relation to ionospheric and solar weather propagation determinants. Signal strength data from seven medium frequency stations of unique transmission locations and varying transmission powers were retrieved in 24-hour segments via a receiving loop antenna, Airspy HF+ Discovery software defined radio, and SDR Sharp software interface network. Retrieved data sets were visualized and analyzed in MATLAB for the identification of signal strength trends, which were subsequently compared to historical ionospheric and space weather indices in pursuit of a quantifiable correlation between such indices and medium frequency signal strengths. The results of the investigation prove that software defined radio, when used in conjunction with a receiving antenna and data analysis program, provides a versatile mechanism for cost-efficient propagation research.

## Keywords

Ionosphere, Space Weather, Airspy SDR, SDR Sharp, MATLAB Analysis

## 1. Introduction

Medium Frequency (MF) radio waves comprise a subsection of the electromag-

netic Radio Frequency (RF) spectrum that contains frequencies between 300 kHz and 3 MHz [1] [2]. In consistency with RF characteristics, the primary utility of MF radio is communication through wave propagation. Common applications of MF radio include AM radio, official government broadcasting, amateur radio, military communications, and communication platforms for emergency response networks [2] [3] [4] [5]. Considering these applications, MF radio maintains relevance amongst modern communication techniques and therefore warrants research efforts that seek to enhance its utility. The ability to consistently and reliably utilize MF radio for communication requires an understanding of the relationship between MF wave propagation modes, ionospheric conditions, and solar weather, all of which influence a signal's ability to travel from the transmitter to the receiver [6]. Traditional characterizations of propagation determinants involve high cost-to-resolution ratios that inhibit research efforts of a more modest scale [7]. Furthermore, though resources exist that define propagation conditions in real-time such as NOAA's DRAP (D-Region Absorption Prediction) and GIRO's (Global Ionospheric Radio Observatory) Ionograms, these resources predominantly characterize the RF High Frequency (HF) range from 3 MHz to 30 MHz [8] [9]. However, the ongoing developments of software-defined radio (SDR) have provided the feasibility of cost-efficient MF data acquisition and subsequent propagation characterization [7]. SDR technology inherently reduces the hardware needed to perform traditional radio functions and simultaneously offers software-derived features that permit structured signal analyses at no additional cost to the user.

Obtaining valid MF propagation data requires a mechanism to perform signal processing, visualization, and data acquisition, all of which are capabilities of SDR technology [7] [10]. Though most consumer SDRs are still dependent on an external connection to an antenna for signal reception and transmission, their primary advantages originate from both back-end and front-end configurability [10] [11]. SDR's incorporation of adjustable hardware such as FPGAs and programmable DSPs allows for back-end modulation configuration around desired signals [10] [11]. Additionally, the "intelligent" or "smart" antennas unique to SDRs extend their receivable frequency range and provide initial compensation for changes in signal properties to enhance received signal quality [10] [11]. Thus, whereas traditional analog radios can offer superiority in two-way communications, modern SDRs with advanced filtering and modulation versatility can maintain or exceed hardware-based radio reception quality [10] [11]. Other SDR features include multi-slice reception, in which multiple frequency ranges can be received simultaneously, and customization of receiving metrics such as bandwidth and filter design [10] [12]. With regard to propagation research, the most significant SDR function is the ability to record received signal data in real-time. Software "plug-ins" such as SDR Sharp's SNR Logger enable an SDR receiving network to function as a comprehensive center for data collection [13]. Given the availability of general data analysis platforms such as MATLAB or Python, SDR's advancements in data acquisition techniques can translate to ad-

vancements in the entire propagation research process.

For this discussion, “characterization” of MF propagation is effectively the definition of numerical relationships between received signal strength and signal attenuation. Signal attenuation, however, has multiple determinants itself, including ionospheric conditions and solar weather events [6] [7]. Increased ionization in the ionosphere, whether it be a product of normal sunlight exposure or abnormal solar activity like a solar flare or coronal mass ejection, will increase attenuation severity. Moreover, propagation can occur through multiple modes of varying paths and distances, subsequently also affecting attenuation [2] [6]. The investigation of interest in this paper includes signal propagation via ground wave (along earth’s surface), sky wave (refraction off the ionosphere), and near-vertical incidence sky wave, or NVIS (near-vertical refraction). With a network of received signals diverse in originating geographic location, transmission power, and propagation path, SDR technology provides a low-cost platform with the versatility for efficient data capture. Finally, evaluation of captured data via data analysis software can yield the numerical relationships between metrics needed to characterize MF signal propagation.

The novelty of this investigation is derived from its simultaneous focus on both the MF signal range and the simplification of the SDR-based research setup. As previously stated, existing propagation characterizations are primarily dedicated to the HF signal range [8] [9]. Thus, propagation research within other signal ranges such as the MF range are principally novel. Furthermore, although this investigation had a conventional technical objective of signal characterization, it explored the novelty of the simplified and cost-efficient method by which that characterization can be obtained—made possible only by recent developments in SDR technology. The work discussed in this paper may more broadly be regarded as an exploration of the increasingly novel utility of SDR technology in a simplified, cost-efficient propagation research methodology.

## **2. Methodology**

Characterization of signal behavior required the following fundamental processes: signal reception, signal processing and formatting, signal strength data collection, and data analysis.

### **2.1. Signal Reception**

#### **2.1.1. Selection of Received Stations**

Because antenna size is inversely proportional to resonant frequency, which is the frequency desired for reception, the initial step towards successful reception was to define the frequencies to be analyzed. Since the purpose of this investigation was to characterize signal strength under fluctuations in propagation conditions, an ideal signal source would have minimal variation in timing and power of transmission. Such properties are possessed by clear-channel AM radio stations, MF beacons, and regulated government broadcasts. Furthermore, selecting multiple geographically diverse stations would ensure diversity of signal propa-

gation via a combination of ground wave, sky wave, and NVIS. As a result, the following stations shown in **Table 1** were selected for reception, data capture, and signal strength analysis.

### 2.1.2. Receiving Hardware

Conventional receiving techniques in RF theory maintain that receiving antennas have a limited effective receivable frequency range as a function of antenna length. While small receiving loop (SRL) antennas are not exempt from this rule, they can offer significant versatility in the quality reception of frequencies in and below the HF band, including the entirety of the MF band. According to antenna theory, small receiving loops can function as the “proper” antenna for electrical lengths that are less than one-tenth of the received signal’s wavelength [14]. Considering the frequencies listed in **Table 1**, an SRL antenna with an electrical length of 12 meters or less would fit the effective receiving range for all stations. Turning to affordable SDR-compatible technology, the SRL of choice was constructed from Airspy’s commercially available “YouLoop HF Loop Antenna.” Although designed to receive HF frequencies, the product contains the equipment necessary to construct loops with electrical lengths of 4, 6, and 8 meters, all of which meet the parameters for quality signal reception of the desired MF frequencies. Consequently, a loop with an electrical length of 4 meters and physical circumference of 2 meters was designated as the official SRL for data collection. It should be noted that the SRL contained a balun transformer on its output to perform initial signal amplification. The balun’s SMA output was connected to a 100 foot section of RG-6 cable via an SMA-to-RG6 adapter. This strictly physical transition between the 50-ohm SMA antenna and the 75-ohm RG6 cable presented an impedance mismatch resulting in a minor signal depreciation from an elevated standing wave ratio (SWR).

## 2.2. Signal Processing and Formatting

The SDR receiver used to process received signals and interface with SDR software was the foundation of the receiving network. In consistency with the focus on affordability and compatibility, the Airspy HF+ Discovery SDR was used for signal processing and data collection. Similar to Airspy’s YouLoop antenna, although designed for HF applications, the functional range of the HF+ Discovery SDR encompasses the MF band [15]. The SDR receiver’s input was the antenna’s RG6 line (again via an RG6-SMA conversion) and the receiver’s output was connected to a standard Lenovo laptop computer via a micro-USB-to-USB cable. As an SDR, the Airspy HF+ Discovery receiver performs all signal processing (e.g., filtering, mixing, IQ reconstruction, and ADC) necessary to obtain an output equivalent to that of traditional hardware-based receivers. Once the hardware connection was established, signal reception was further configured with the SDR software platform SDR Sharp (SDR#). SDR Sharp was chosen amongst a multitude of viable SDR platforms for its known Airspy compatibility, configuration versatility, and data acquisition capabilities with multi-frequency slicing and signal strength logging.

**Table 1.** MF stations received and analyzed.

Station Call	Station Type	Transmitter Location	Frequency (kHz)	Transmission Power (W)
WBZ	AM Broadcast	Boston, MA	1030	50,000
WLS	AM Broadcast	Chicago, IL	890	50,000
KYW	AM Broadcast	Philadelphia, PA	1060	50,000
WBAL	AM Broadcast	Baltimore, MD	1090	50,000
CHLO	AM Broadcast	Brampton, Ont. (Canada)	530	1000 at Day 250 at Night
RNB	Beacon	Millville, NJ	363	150
WWV	NIST Broadcast	Fort Collins, CO	2500	2500

\*Receiving station was located in Annville, PA. Transmission information obtained from [3] [4] [5].

### 2.3. Signal Strength Data Collection

All data collection was accomplished with an additional function or “plug-in” in SDR Sharp known as the SNR Logger. The SNR Logger calculates and writes to a CSV file the peak signal strength, noise floor, and SNR (signal-to-noise ratio) of the received signal within a user-defined bandwidth. Although nearly all front-end SDR settings can affect the final signal logged by the SNR Logger, trial tests determined that receive bandwidth, preamplification, automatic gain control (AGC), and logging rate held a dominant influence on the resulting data. Thus, to obtain logged signal strengths with minimal error, all four factors were minimized such that preamplification and AGC were disabled, bandwidths were set to 100 Hz, and the logging rate was defined as one sample per second.

Data acquisition efficiency was maximized through the utilization of SDR Sharp’s slicing capability, which allows the user to simultaneously open multiple windows or “slices” with unique receiving frequencies. Each slice retains a portion of the configuration options of the master interface, including the ability to activate plug-ins such as the SNR Logger. Hardware limitations of the SDR Sharp host computer restricted the maximum number of concurrent slices to five. Therefore, data acquisition consisted of the simultaneous reception and signal strength logging of five individual stations. Signal logging was performed in 24-hour sections and multi-day streaks during periods with both forecasted space weather activity and undisturbed conditions. Logging durations of 24-hour multiples were chosen to ensure capture of the full ionospheric fluctuations that occur at the same rate. Under normal solar activity, the ionosphere exhibits four main phases: high ionization during the daytime, low ionization during the nighttime, and a transitional rise and fall as the sun rises and sets, respectively. A continuous operation was needed to capture data throughout all phases, so it was necessary to indefinitely charge the SDR Sharp host computer. The ambient noise floor was subsequently elevated by 15 dB for all data acquisitions because

of the charger connection, but the peak signal strength (the measurement of interest) remained unaffected.

## **2.4. Data Analysis**

### **2.4.1. Standard Visualization Technique**

The data analysis process was initiated via the SNR Logger function in SDR Sharp. At the conclusion of a data capture period the signal strength data for each frequency could be accessed in an auto-populated CSV file with preformatted individual columns for timestamp (EDT), frequency (Hz), noise floor (dB), SNR (dB), and peak signal strength (dB). Although any primary coding platform would have offered the tools necessary to perform data visualizations and numerical analyses, MATLAB was selected for its ease of data navigation and RF-related toolboxes. Visualization was made the first step towards achieving concrete characterization because it provided a method of observing signal behavior over a 24-hour period in a single figure. Thus, a basic scatter plot was produced for the signal strength data in the time domain for each 24-hour period. This visualization technique allowed an initial assessment of the data's validity to be performed prior to any numerical calculations in which invalid behavior may have been unobservable. Once the basic scatter plot was established, vertical lines for the official sunset and sunrise times at both the receiving station and transmitting station were imposed to help visualize relative trends. Consideration for the sunset and sunrise at both locations was necessary since ionospheric ionization is relative to sunlight exposure and sunlight exposure is relative to geographic location. The imposition of sunset and sunrise lines was one method of visually identifying periods of known changes in ionization that could be conducive for empirical analyses.

### **2.4.2. Empirical Analyses**

Empirical analyses of the signal strength data were designed to define numerical relationships between received signal strength (in dB) and measurable propagation determinants. Analyses were conducted in the three step process of observe, quantify, and correlate. While "observe" was accomplished via the time domain scatter plot, quantification of signal behavior was broken into two approaches: rapid change analysis and ionospheric phase analysis. Rapid change analysis focused on identifying sudden significant fades or peaks in signal strength. Since the definitions of "sudden" and "significant" are subjective, appropriate values for time and severity were estimated based on a listener's reception of the signal. As a result, a "rapid change" was deemed to be a peak signal strength change of 18 dB or more within the duration of one minute. This analysis was designed to identify the impacts of solar weather events, which can rapidly increase ionization in the ionosphere, increasing MF signal attenuation and decreasing received signal strength. The analysis was implemented with a "scrolling window" technique, such that each possible one-minute section of consecutive signal strength data points was evaluated. For each section, the range between the maximum

signal strength and minimum signal strength was calculated and used to determine whether that section contained a “rapid change.” Finally, the timestamps and exact range were retrieved in a tabular format for all rapid changes.

Conversely, ionospheric phase analysis considered the four major ionospheric phases. As periods of relatively constant ionospheric stability, the daytime and nighttime regions were characterized by an average signal strength value. The transition regions around sunset and sunrise, which were respectively observed as a rise and fall in signal strength, were characterized by the severity of that rise or fall (*i.e.*, the slope) in terms of dB per minute. This analysis was favorable for comparisons between propagation modes (e.g., sky wave vs. NVIS) and daily variations in indices with extended ionospheric effects like electron density levels. An ideal application of ionospheric phase analysis would identify a significant change in either the average value or slope of the signal strength data and correlate the change to a proportional shift in an ionization determinant. The data analysis methodology was dependent on the realization of two factors: observable anomalies in signal strength behavior and the identification of correlated ionospheric indices. “Indices” were regarded as measurable metrics of ionization, the ionosphere, solar weather, and their determinants [16] [17] [18] [19]. Databases from organizations such as NOAA and GIRO were consulted for such information. However, priority was given to solar weather events and their expected effects of rapid changes in MF signal strength [1] [16] [17] [18] [19]. The signal acquisition and analysis methodology is summarized below in **Figure 1**.

### 3. Results

#### 3.1. Observation

First, the accuracy of the data acquisition system was validated through the alignment of signal behavior with ionospheric phases. Just as the ionosphere transitions between four general phases of differing ionization levels in a 24-hour cycle, the 24-hour signal strength plots for each station exhibited four clear phases: a daytime low, an evening rise, a steady overnight high, and a morning fade back to the daytime low. This general shape was observed for all seven stations regardless of their differences in propagation modes. For example, while the signal data in **Figure 2** would have traveled to the receiver via sky wave, the signal data in **Figure 3** would have traveled via a combination of ground wave and NVIS. Despite the visual difference from the absence/presence of ground wave, the consistent appearance of the four-phase shape allowed it to be regarded as a neutral baseline from which deviations could be subsequently regarded as anomalies.

#### 3.2. Quantification

**Figure 4** displays an example of a rapid change analysis. Though the purpose of such an analysis was to characterize periods of high volatility, quantification of



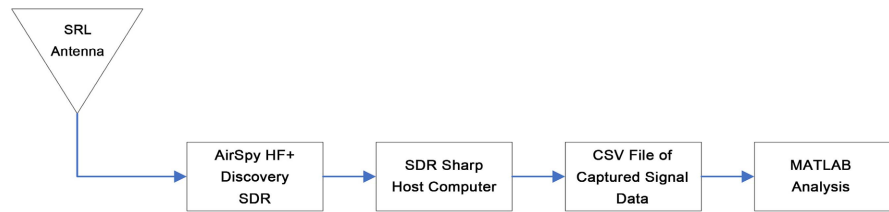


**Figure 1.** Signal data acquisition and analysis methodology.

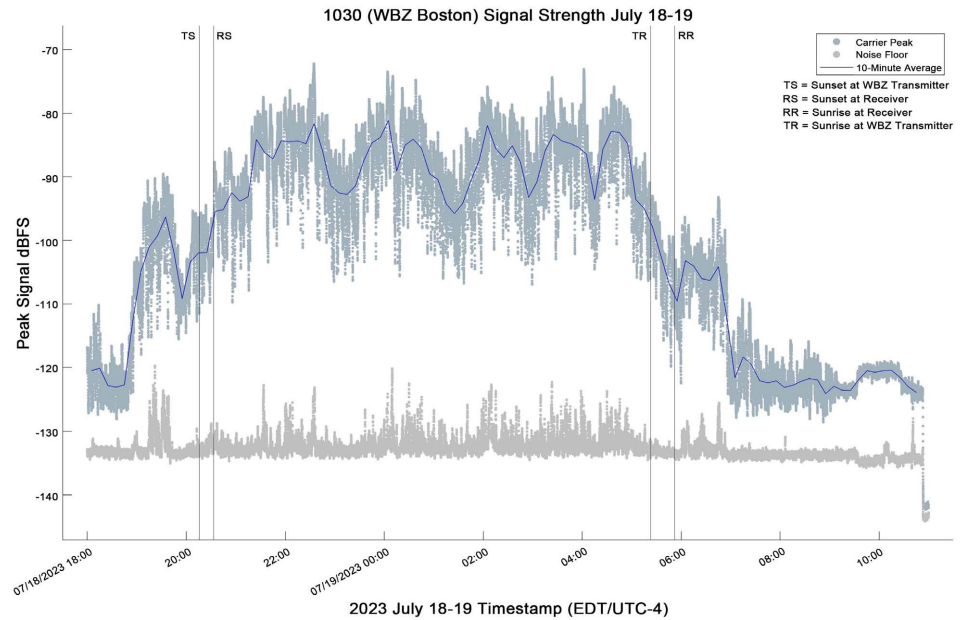


**Figure 2.** Received signal strength for 1030 KHz (WBZ Boston) overnight from July 18 to July 19, 2023.

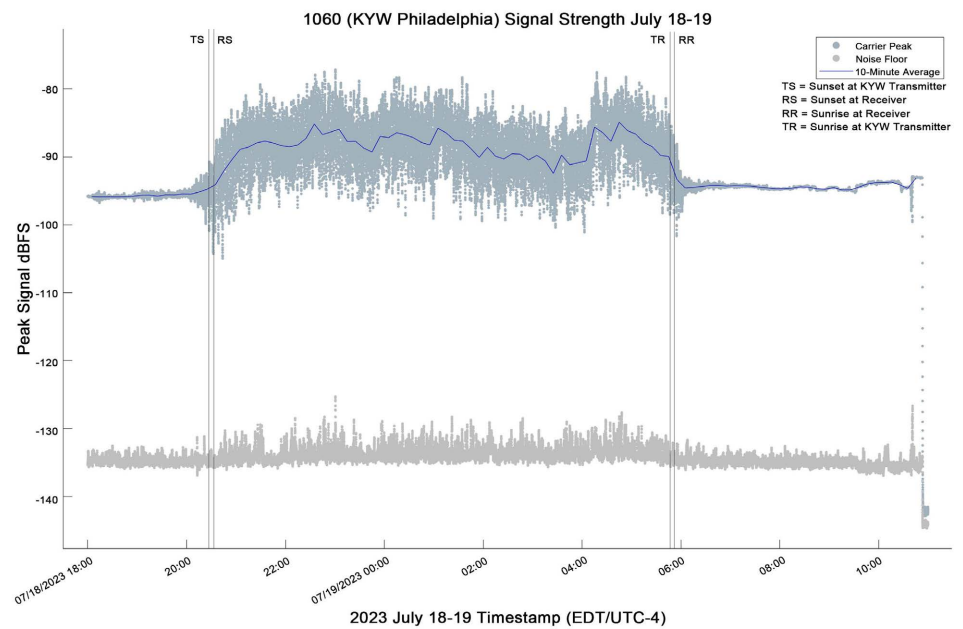


**Figure 3.** Received signal strength for 1060 KHz (KYW Philadelphia) overnight from July 18 to July 19, 2023.



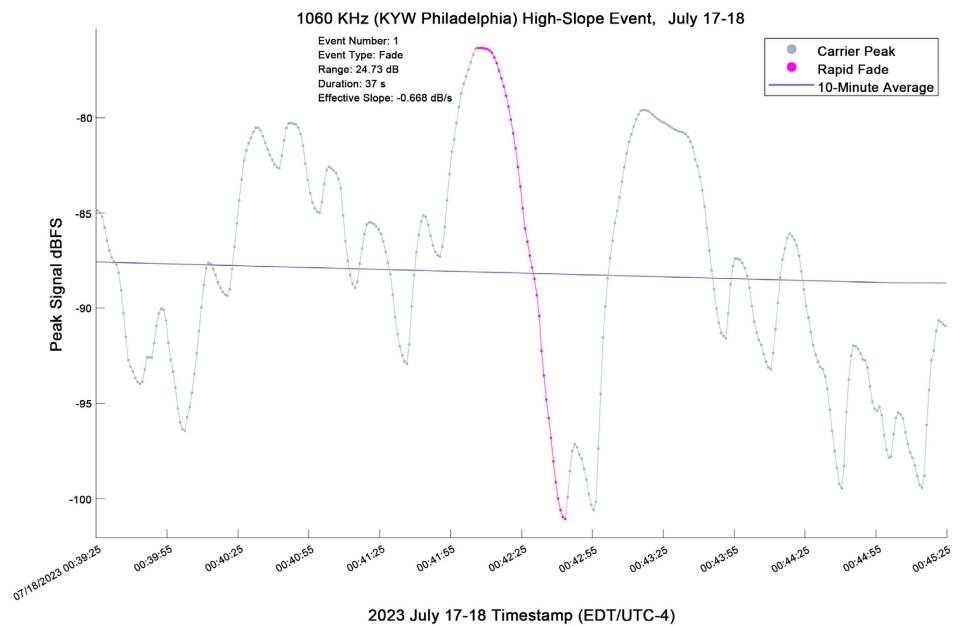


**Figure 4.** Example of rapid change analysis.

that volatility revealed that changes of 18 dB or more in less than one minute were not uncharacteristic of normal signal behavior. This was especially true for signals that relied on sky wave propagation (*i.e.*, those being transmitted from over 150 miles away), as their absence of ground wave caused routine refractive losses to become losses of the majority of the signal.

**Figure 5** shows an example of the general graphical behavior that the ionospheric phase analysis quantified. Consecutive 24-hour periods were compared to identify solar events with a less severe or prolonged ionospheric impact. With reference to **Figure 5**, the “Overnight Rise Slope” and “Morning Fade Slope” were calculated metrics similar to the “Effective Slope” value in **Figure 4**.

**Figure 6** is an example of another quantification technique: the calculation of a signal’s mean overnight strength. Quantified changes in overnight average signal strength would aid in defining a numerical relationship between signal strength and a correlated ionization determinant. The quantification techniques described above were applied to all 24-hour and multi-day plots of signal data.

### 3.3. Correlation

The final step in characterizing a relationship between the quantified MF signal behavior and an element of ionospheric conditions was identifying an ionospheric or space weather determinant that correlated to abnormal signal behavior. This was inhibited by two factors: 1) lack of recorded abnormal signal behavior, and 2) lack of consistent correlation across multiple data sets. While solar weather events did occur during data acquisition, the corresponding signal data did not exhibit any abnormalities beyond what would be attributable to the effects of normal attenuation, instrument error, and transmission fluctuations. On occasion, minor correlations were identified for multi-hour sections of the

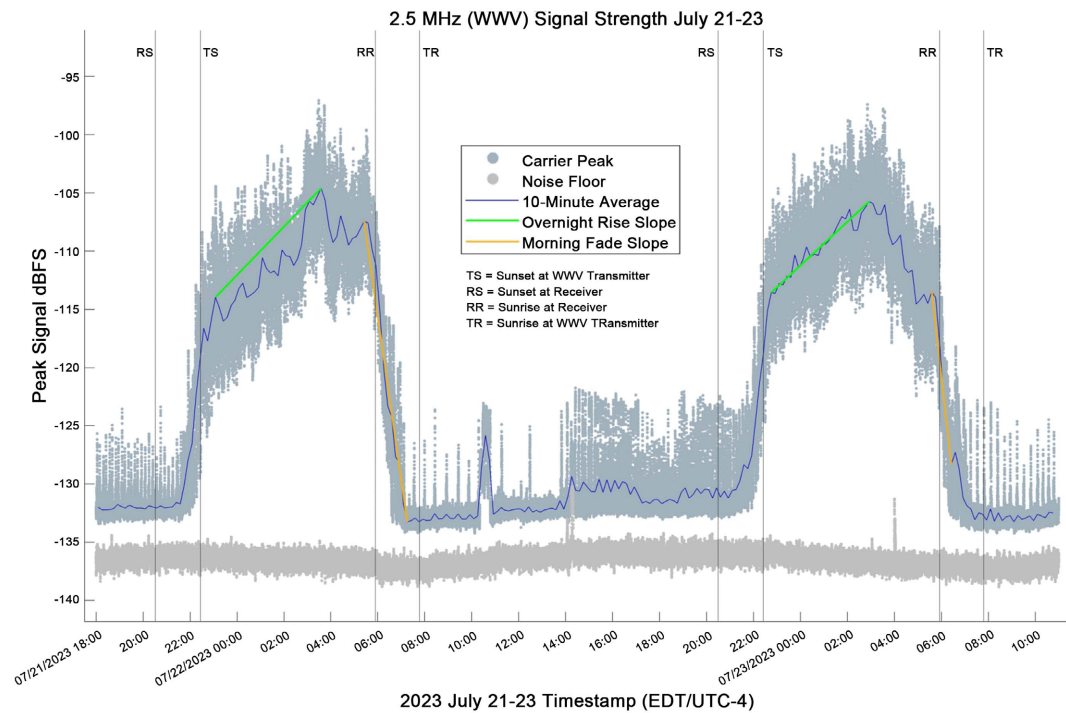


**Figure 5.** Example of ionospheric phase analysis for rising and falling slopes.

Sunset_to_Sunrise	WWV_Overnight_Mean	WWV_diff
21-Jul-2023 to 22-Jul-2023	-116.65	NaN
22-Jul-2023 to 23-Jul-2023	-116.46	0.18241
23-Jul-2023 to 24-Jul-2023	-117.06	-0.59278

**Figure 6.** Example of ionospheric phase analysis for overnight average signal strength. The rightmost two columns are in units of decibels (dB).

data received from a single station, but the same correlations were not maintained for the other stations. Because of these two factors, a definitive numerical relationship between MF signal strength and ionospheric or space weather metrics was not identified.

#### 4. Conclusion

Though a concrete correlation equation between signal strength and an ionization determinant was not identified, the utility of SDR as a mechanism for low-cost propagation research is supported. SDRs, and in particular the combination of the Airspy HF+ Discovery hardware and SDR Sharp software, provide the configurability, extended reception range, and data acquisition tools necessary to function as a comprehensive signal data acquisition device. The results of this investigation were limited by its scope, and the SDR had no contribution to the lack of MF signal characterization. A more involved effort with a greater emphasis on historical data base research and correlation identification could achieve the desired level of characterization. Nonetheless, SDR remains an op-

timal choice for low-cost signal reception, reception configurability, and data acquisition.

## 5. Future Recommendations

Improvements can be made to this system's hardware setup, software configuration, and data analysis approaches. First, it was previously noted that the signal noise floor was elevated by roughly 15 dB because the SDR Sharp host computer needed constant charging. To remove this unwanted noise, it is recommended that the SDR Sharp host machine be powered by battery to eliminate sources of AC noise. The high watt-hour ratings and relatively small size of LiFePO<sub>4</sub> batteries make them a viable power source. For software configuration, it is recommended that any settings related to amplification or manipulation of the raw received signal be turned off or disabled. SDR Sharp is not the only viable SDR configuration software, so any changes in software would require a new settings configuration to record the raw received signal, which is an effective method of normalizing signal data between software platforms. Lastly, the data acquisition and analyses in this investigation were in the time domain. If signal characterization is the ultimate goal, it is recommended that data also be taken from the frequency domain to visualize trends not visible in the time domain. This could be accomplished by implementing a high-resolution oscillator, either as a single additional component or within a more advanced SDR, against which the frequency of received signals could be measured. However, it was determined that the addition of a reference oscillator would have been out of scope for this investigation's focuses on cost-efficiency, simplicity, and SDR versatility.

## Conflicts of Interest

The authors declare no conflicts of interest regarding the publication of this paper.

## References

- [1] Frissell, N.A., Miller, E.S., Kaeppler, S.R., Ceglia, F., Pascoe, D., Sinanis, N., Smith, P., Williams, R. and Shovkoplyas, A. (2014) Ionospheric Sounding Using Real-Time Amateur Radio Reporting Networks. *Space Weather*, **12**, 651-656. <https://doi.org/10.1002/2014SW001132>
- [2] Levis, C.A., Johnson, J.T. and Teixeira, F.L. (2010) Radiowave Propagation: Physics and Applications. <http://ci.nii.ac.jp/ncid/BB03015333>
- [3] Hepburn, W. (2023) LW Radio Beacons. <https://www.dxinfocentre.com/ndb.htm>
- [4] NIST (2023) Radio Station WWV. <https://www.nist.gov/pml/time-and-frequency-division/time-distribution/radio-station-wwv>
- [5] Federal Communications Commission. AM Station Classes, and Clear, Regional, and Local Channels. <https://www.fcc.gov/media/radio/am-clear-regional-local-channels>
- [6] Crane, R.K. (1981) Fundamental Limitations Caused by RF Propagation. *Proceedings of the IEEE*, **69**, 196-209. <https://doi.org/10.1109/PROC.1981.11952>

- [7] Hanbali, S.B.S. (2023) Low-Cost Software-Defined Radio for Electrical Engineering Education. *IEEE Potentials*, **42**, 13-19. <https://doi.org/10.1109/MPOT.2022.3223788>
- [8] NOAA/NWS Space Weather Prediction Center. Global D-Region Absorption Prediction Documentation. <https://www.swpc.noaa.gov/content/global-d-region-absorption-prediction-Docum entation>
- [9] Reinisch, B.W. and Galkin, I.A. (2011) Global Ionospheric Radio Observatory (GIRO). *Earth, Planets and Space*, **63**, 377-381. <https://doi.org/10.5047/eps.2011.03.001>
- [10] Sinha, D., Verma, A. and Kumar, S. (2016) Software Defined Radio: Operation, Challenges and Possible Solutions. 10<sup>th</sup> *International Conference on Intelligent Systems and Control (ISCO)*, Coimbatore, 7-8 January 2016, 1-5. <https://doi.org/10.1109/ISCO.2016.7727079>
- [11] Akeela, R. and Dezfouli, B. (2018) Software-Defined Radios: Architecture, State-of-the-Art, and Challenges. *Computer Communications*, **128**, 106-125. <https://doi.org/10.1016/j.comcom.2018.07.012>
- [12] Cruz, P., Carvalho, N.B. and Remley, K.A. (2010) Designing and Testing Software-Defined Radios. *IEEE Microwave Magazine*, **11**, 83-94. <https://doi.org/10.1109/MMM.2010.936493>
- [13] Diaz-Ortiz, F., Roman, F., Lopez, J. and Gomez, C. (2016) High-Speed Data Acquisition System for Radio Atmospheric Signals Measurements Based on Software Defined Radio. 2016 33rd *International Conference on Lightning Protection (ICLP)*, Estoril, 25-30 September 2016, 1-4. <https://ieeexplore.ieee.org/stamp/stamp.jsp?tp=&arnumber=7791426>
- [14] Breed, G. (2007) Basic Principles of Electrically Small Antennas. *High Frequency Electronics*, **6**, No. 2. [https://www.highfrequencyelectronics.com/Feb07/HFE0207\\_tutorial.pdf](https://www.highfrequencyelectronics.com/Feb07/HFE0207_tutorial.pdf)
- [15] Airspy.com. Try Our Award Winning HF/VHF Receiver! <https://airspy.com/airspy-hf-discovery/>
- [16] Poole, I. (1999) Radio Waves and the Ionosphere. <https://www.arrl.org/files/file/Technology/pdf/119962.pdf>
- [17] Poole, I. (2002) Understanding Solar Indices. QST © ARRL, 38-40. <https://www.arrl.org/files/file/Technology/tis/info/pdf/0209038.pdf>
- [18] Otsuka, Y., Jin, H., Shinagawa, H., Hosokawa, K. and Tsuda, T. (2023) Ionospheric Variability. In: Kusano, K., Ed., *Solar-Terrestrial Environmental Prediction*, Springer, Singapore. [https://doi.org/10.1007/978-981-19-7765-7\\_7](https://doi.org/10.1007/978-981-19-7765-7_7)
- [19] Murase, K., *et al.* (2023) Atmospheric Ionizations by Solar X-Rays, Solar Protons, and Radiation Belt Electrons in September 2017 Space Weather Event. *Space Weather*, **21**, e2023SW003651. <https://doi.org/10.1029/2023SW003651>